

Article

Design, DEM Simulation, and Field Experiments of a Novel Precision Seeder for Dry Direct-Seeded Rice with Film Mulching

Hui Li ^{1,2}, Shan Zeng ¹, Xiwen Luo ^{1,2}, Longyu Fang ², Zhanhao Liang ¹ and Wenwu Yang ^{1,*}

¹ Key Laboratory of Key Technology on Agricultural Machine and Equipment, Ministry of Education, South China Agricultural University, Guangzhou 510642, China; lihui17@mails.jlu.edu.cn (H.L.); shanzeng@scau.edu.cn (S.Z.); xwluo@scau.edu.cn (X.L.); lz kou@stu.scau.edu.cn (Z.L.)

² College of Biological and Agricultural Engineering, Jilin University, Changchun 130022, China; fangly20@mails.jlu.edu.cn

* Correspondence: yangwenwu@scau.edu.cn

Abstract: Existing devices for dry direct-seeded rice with film mulching in northern China have limitations such as imprecise sowing, unadjustable sowing depth, and seeding device blocking. In this regard, this study proposes a combined seeding method of ‘mini shovel + telescopic pipe’ for dry direct-seeded rice with film mulching. A precision seeder for dry direct-seeded rice with film mulching was developed through theoretical calculations, discrete element modelling (DEM) simulations, and field experiments. The configuration and diameter of the rollers were obtained. Twelve telescopic pipes were evenly distributed on the circumference of the roller, with a contact ratio exceeding one. This ratio reduced the slip rate of the roller effectively. Subsequently, DEM was used to develop a 3³ central composite design. The response surface was established with the sowing depth as the response value. According to agronomic requirements, the sowing depth was set to 20 mm. The optimal combination of working parameters was obtained by optimizing the regression equation. The field experiments showed that the performance of the precision seeder for dry direct-seeded rice with film mulching satisfied the requirements of agricultural production, working stably and reliably. The developed device represents a useful solution for dry direct-seeded rice with film mulching.

Keywords: film mulching; mini shovel; telescopic pipe; discrete element modelling; hill-drop sowing



check for updates

Citation: Li, H.; Zeng, S.; Luo, X.; Fang, L.; Liang, Z.; Yang, W. Design, DEM Simulation, and Field Experiments of a Novel Precision Seeder for Dry Direct-Seeded Rice with Film Mulching. *Agriculture* **2021**, *11*, 378. <https://doi.org/10.3390/agriculture11050378>

Academic Editor: José Pérez-Alonso

Received: 28 March 2021

Accepted: 19 April 2021

Published: 21 April 2021

Publisher's Note: MDPI stays neutral with regard to jurisdictional claims in published maps and institutional affiliations.



Copyright: © 2021 by the authors. Licensee MDPI, Basel, Switzerland. This article is an open access article distributed under the terms and conditions of the Creative Commons Attribution (CC BY) license (<https://creativecommons.org/licenses/by/4.0/>).

1. Introduction

Rice transplanting is a conventional rice cultivation technology in Asia consisting of four basic steps: nursery bed preparation, seedling raising, seedling uprooting, and transplanting the seedling into the field. All of these steps are highly labor-intensive and water-intensive [1,2]. However, with the rapid economic development in China, the phenomenon of labor shortage appears, leading to the rising of labor wages and production cost in agriculture. Thus, rice production is becoming less profitable [3]. Furthermore, water scarcity is becoming more severe and widespread for rice cultivation [4]. Direct-seeded rice is a feasible alternative method to deal with the shortages of water and labor [5]. Direct-seeded rice consists of directly sowing seeds into the field and represents a simplified cultivation technology, which is a trend toward the future of rice cultivation [6–8]. Xu et al. [9] compared the effects of rice transplanting and direct-seeding rice on yield. The results showed that direct-seeding rice could produce comparable yields to rice transplanting, but direct-seeded rice was exposed to more risks such as weed encroachment and extreme weather. Kakumanu et al. [10] reported that direct-seeded rice was efficient in terms of reducing impacts of climate, water use, increasing grain yield, and better returns to farmers.

In recent years, dry direct-seeded rice with film mulching technique has been adopted to improve water utilization rate, reduce herbicide usage, and improve soil temperature after sowing in rice areas of northern China, which could effectively solve and mitigate the risk of direct-seeding rice [11–13]. Jabran et al. [14] reported that plastic film mulching improved the soil moisture retention, and enhanced rice water productivity, grain yield, and rice quality. Li et al. [15] showed that plastic film mulching with no flooding could provide higher rice yield under appropriate water condition and change the soil nutrient cycle. Row drilling and hill-drop drilling are the main sowing methods for direct-seeded rice. Specifically, hill-drop drilling is beneficial for improving field permeability, leaf photosynthesis, and photosynthetic productivity [16,17]. In this regard, hill-drop drilling is the better sowing method for dry direct-seeded rice with the film mulching technique due to its low film-breaking rate.

Currently, the dry direct-seeded rice with film mulching devices are mainly based on the duckbill-type roller seeder, which is a modified design from seeders for other crops, such as wheat and corn seeders. However, these devices cannot obtain precise seeding because of the differences between rice and other crops in terms of the flowability and triaxial size of seeds. The duckbill-type seed-metering device has a disadvantage: the sowing depth cannot be adjusted. Moreover, stone and caking soil are present in seeding beds in some parts of northern China, causing obstructions in the duckbill-type seed-metering device, leading to miss-seeding, reseeding, or even sparse failures, which seriously affect the rice yield. Various studies have been conducted to solve or mitigate the risks of the duckbill-type seeder. A CAM mechanism was added into the duckbill-type seed-metering device to change the passive opening into the active aperture of the seed-metering device, which alleviated the miss-seeding caused by the failure of the duckbill-type seeder to open in the case of hard objects [18]. The length and shape of the duckbill seeder were optimized to reduce the size of the film hole and avoid the formation of plastic film hanging on the duckbill-type seeder [19]. The internal seed-taking structure of the duckbill-type seeder was optimized, improving the seeding accuracy [20]. All the above studies have played a positive role in improving the performance of the duckbill-type roller seeder, achieving good results. However, the problems such as blocking of the duckbill seeder and inability to adjust the sowing depth remain unsolved.

In this study, to overcome these limitations, the ‘mini shovel + telescopic pipe’ combination-seeding method was proposed, and a precision seeder for dry direct-seeded rice with film mulching was developed. The mechanism was developed based on the previous studies and through the analysis of the traditional artificial sowing process (including three steps: dig a hole with a shovel → seed pitching by reaching out hand → take back hand and shovel) and considering the technique of seeding in dry soil and drip irrigation for emergence.

The proposed rice precision seeder combines a type-hole seed-metering device to realise precision sowing and adjust the seeding quantities [21,22]. The mini shovel pushes aside the soil and hard materials within the seeding area to form a cavity. Subsequently, the telescopic pipe stretches out like a hand to cast seeds, which effectively prevent the telescopic pipe from being blocked. The extension length of the telescopic pipe controls the sowing depth adjustment by changing the upper and lower position of the drive slideway. Optimal design of the critical component was conducted, and experimental analysis of the working performance and operation effect was performed to obtain the optimal combination of working parameters. The field experiments contribute to providing a new machine for dry direct-seeded rice with film mulching of high quality, without blockage of the telescopic pipe, as well as the development of precision agriculture.

2. Structure and Working Principles of the Proposed Seeder

2.1. Machine Structure

Figure 1 illustrates the overall structure of the developed precision seeder for dry direct-seeded rice with film mulching. The rice precision seeder consists of frame, suspen-

sion system, control, drive systems, combined type-hole seed-metering device, roller, mini shovel, telescopic pipe, and other key components.

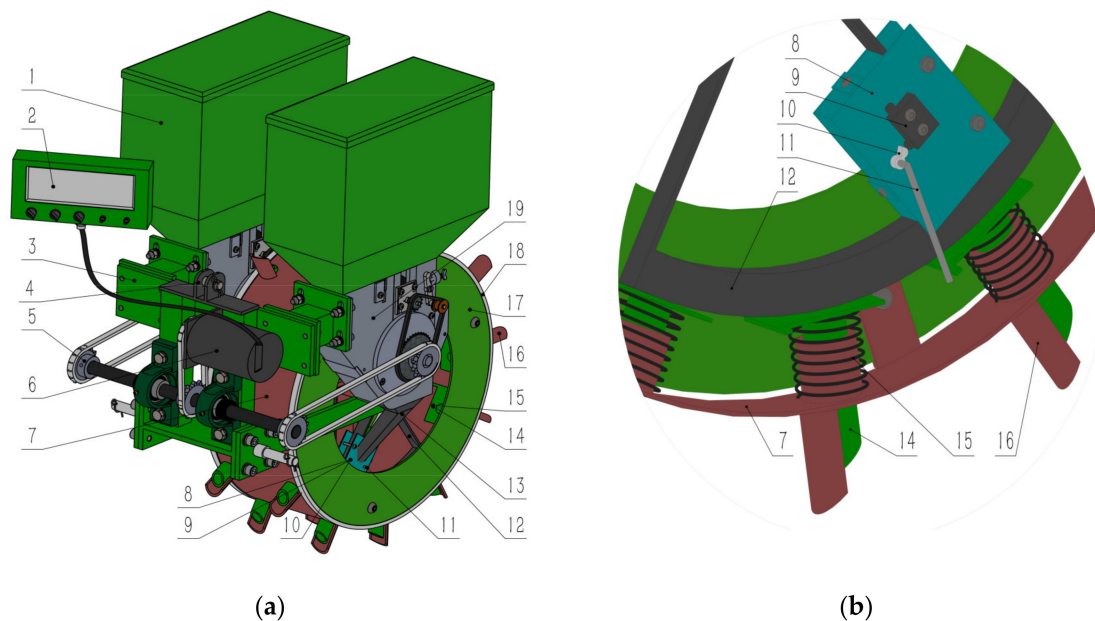


Figure 1. 3D model of the novel precision seeder for dry direct-seeded rice with film mulching: (a) Axonometric drawing of the entire machine; (b) Partial enlarged view. 1. Seed tank 2. Control box 3. Frame 4. Suspension system 5. Chain drive system 6. Stepping motor 7. Roller 8. Dividing seeds box 9. Touch switch 10. Micro CAM 11. Crank 12. Drive slideway 13. Seed tube 14. Telescopic pipe 15. Reset spring 16. Mini shovel 17. Protection plate 18. Rubber ring 19. Combined type-hole seed-metering device.

2.2. Working Principle

The precision seeder for dry direct-seeded rice with film mulching has two rows, which are connected to the traction device using a trifilar suspension system. The movement of the traction device drives the roller rotation, and the mini shovel enters the soil as the roller rotates. The soil and hard materials within the seeding area are pushed aside to form a cavity simultaneously, and the telescopic pipe sticks out under the action of the drive slideway. Seeds are dropped into the cavity through the telescopic pipe after the top end of the telescopic pipe touches the crank. The crank drives the micro CAM to rotate so that the touch switch is on. The control system commands the stepping motor to drive the combined type-hole seed-metering device to rotate 45° to seed to the dividing seeds box for the next sowing. After sowing, the telescopic pipe returns quickly to detach the adhesive attachment under the action of the reset spring. The mini shovel leaves the soil, and the seeding operation finishes. The extension length of the telescopic pipe controls the sowing depth adjustment by changing the upper and lower position of the drive slideway.

2.3. Structural Design of Critical Component

2.3.1. Roller and Contact Ratio

The roller is the supporting part of the seed-throwing mechanism and provides power for moving components. According to the preliminary experiments and referring to previous studies, the diameter of the roller was selected as 410 mm [23–25]. The agronomic requirement of holes distance is 140 ± 10 mm. According to the preliminary simulated experiments, the length of the mini shovel is 70 mm, which can satisfy the seeding performance and increase the roller torque; thus,

$$N = \pi(D + 2H)/s \quad (1)$$

N —Number of mini shovels;

D —Diameter of the roller, mm;
 H —Length of the mini shovel, mm;
 S —Hole spacing, mm.

Substituting the parameters into Equation (1), considering $N = 12.3$, rounded to $N = 12$, and isolating the holes distance separation from Equation (1), a hole spacing of $S = 143.9$ mm is obtained, which satisfies the agronomic requirements of holes distance.

A certain sliding phenomenon exists in the operation of the roller; that is, the roller changes from rotating to sliding, which will affect the stability of the holes distance separation and reduce the performance of the device. The slip rate of the roller will reduce if a certain degree of contact ratio between the mini shovels and the soil is present. As shown in Figure 2., point A is the entry point, while point B is the exit point. The contact ratio (ϵ) is the ratio of the mini shovel angle of rotation ($\theta_1 + \theta_2$) to the center angle corresponding to two adjacent mini shovels (θ_0). If the contact ratio (ϵ) is higher than one, the slip rate will reduce, and the adverse effects will reduce.

$$\theta_1 = \theta_2 = \cos^{-1} \frac{R}{R + H} \tag{2}$$

$$\theta_0 = \frac{2\pi}{N} \tag{3}$$

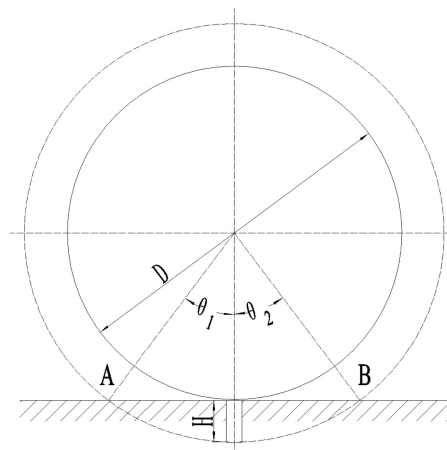


Figure 2. The contact ratio of the mini shovels.

Then:

$$\epsilon = \frac{\theta_1 + \theta_2}{\theta_0} = \frac{N}{\pi} \cos^{-1} \frac{R}{R + H} \tag{4}$$

θ_0 —Center angle, °;
 θ_1, θ_2 —Angle of rotation of the mini shovel;
 ϵ —Contact ratio;
 N —Number of mini shovels;
 R —Roller radius ($D/2$), mm;
 H —Length of mini shovel, mm.

The parameters R, H and N are substituted into the above equation; thus, $\epsilon = 2.7868 > 1$.

The contact ratio is $\epsilon = 2.7868 > 1$ when the roller diameter is 410 mm, the number of mini shovels is 12, and the length of each mini shovel is 70 mm. These parameters provide a useful configuration to reduce the slip rate of the roller and ensure stable holes distance separation.

2.3.2. Drive Slideway

The drive slideway is the core part of the device that ensures the stable displacement of the telescopic pipe and adjusts the extension length of the telescopic pipe; that is, the

sowing depth. According to its function, the drive slideway can be divided into two parts: the drive and holding sections.

When the telescopic pipe touches the drive slideway in the drive section, it gradually stretches out during the roller rotation. The telescopic pipe moves following the spiral of the law of Archimedes. The position equation of the contact point between the telescopic pipe and the drive slideway is:

$$\begin{cases} x = [85 + 0.5(\theta - 15)] \cos \theta \\ y = [85 + 0.5(\theta - 15)] \sin \theta + (35 - H_1) \end{cases} \quad (5)$$

θ —Angle of rotation of the telescopic pipe, $^\circ$, $\theta \in [15, 220]$;

x, y —mm;

H_1 —Telescopic pipe stretching out length, mm.

The telescopic pipe rotates with the roller and no longer extends in the holding section, thus, maintaining a fixed extended length. As shown in Figure 2, this section is mainly the interval between the entry point A and the exit point B; the position equation of the contact point between the telescopic pipe and the drive slideway is:

$$\begin{cases} x = 180 \cos \theta \\ y = 180 \sin \theta + (35 - H_1) \end{cases} \quad (6)$$

θ —Angle of rotation of the telescopic pipe, $^\circ$, $\theta \in [220, 300]$;

x, y —mm;

H_1 —Telescopic pipe stretching out length, mm.

The smooth extension and small vibration impact of the telescopic pipe driven by the drive slideway is an essential performance of the drive slideway, which guarantees the operation quality. In this study, motion simulation function in SolidWorks is used to perform kinematic analysis of the operation process. The preset extended length of the telescopic pipe is 35 mm, the forward speed of the traction device is 0.4 m/s, and the motion curve of the telescopic pipe is shown in Figure 3.

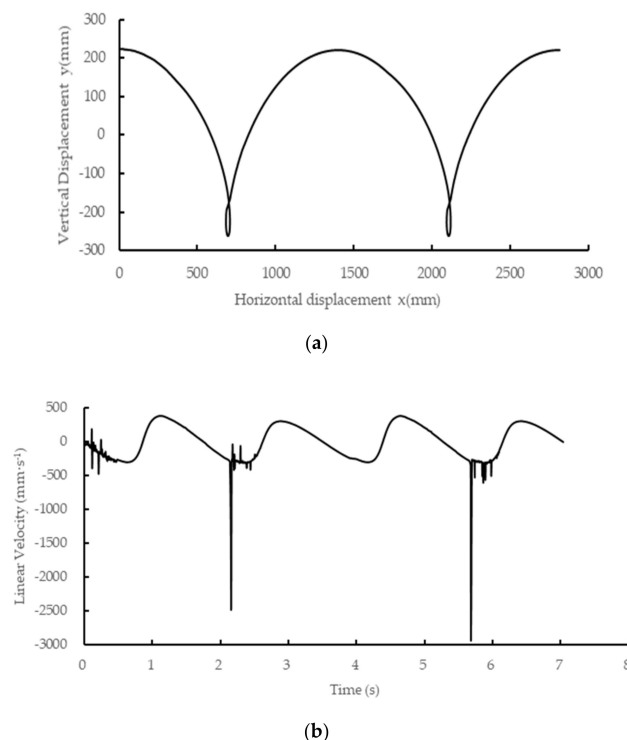


Figure 3. The motion curve of the telescopic pipe: (a) The path of the telescopic pipe; (b) Linear velocity radial component of the telescopic pipe.

As shown in Figure 3a, the motion path of the telescopic pipe under the preset motion condition is smooth, with a convex point in the return, which is basically consistent with the design goal. The convex point is due to the rapid return of the telescopic pipe under the action of the reset spring when it detaches from the drive slideway.

As shown in Figure 3b, velocity bulges are visible near the starting point and the point the telescopic pipe detaches from the drive slideway. Except for that, the change in velocity is flat without sudden impacts; thus, the vibration is reduced to a certain extent, and the seeder reliability and sowing quality are effectively guaranteed.

2.3.3. Mini Shovel and Telescopic Pipe

The mini shovel and telescopic pipe are crucial parts in contact with the soil, which directly determine the performance of the device. The mini shovel has two functions: pushing aside the soil and hard materials within the seeding area to form a cavity and increasing the torque of the roller. The structure and size of the mini shovel are obtained according to experience and pre-tests, as shown in Figure 4a. The arc at the top of the mini shovel helps to cut the mulch film and reduce the possibility of scraping the mulch film.

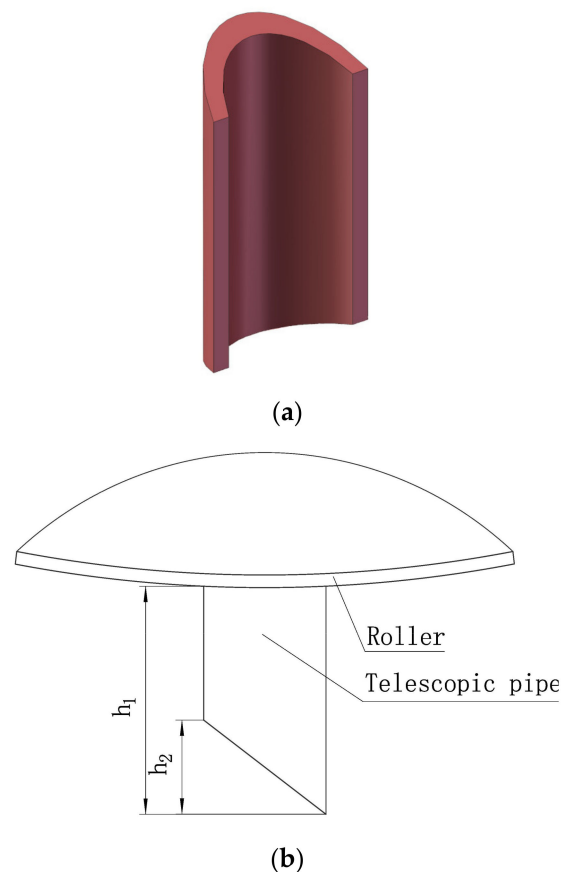


Figure 4. The seeds throwing mechanism: (a) Mini shovel; (b) The structure of telescopic pipe.

The telescopic pipe is the part performing the sowing, and the extended length of the telescopic pipe determines the sowing depth, as shown in Figure 4b. However, it is not equal to the sowing depth. The sowing depth is related to factors such as the forward speed of the traction device, the extended length of the telescopic pipe, the height of the lower oblique section of the telescopic pipe, and the soil characteristics. Thus, determining the parameters of the telescopic pipe is a complicated process. No accurate model can directly determine the optimal values of these parameters; therefore, the discrete element method (DEM) is used to simulate and analyze the operation process of the telescopic pipe. Section 3.1 presents the detailed information and procedures used in this study.

2.3.4. Electronic Control System

The electronic control system is an essential part of the device that directly affects the performance of the machine. Eight holes are evenly distributed on the wheel circumference of the combined type-hole seed-metering device. The average center angle is 45°, that is, rotating 45° to sow once. As shown in Figure 5, this study considers an MCU (single-chip microcomputer) as the control core to ensure the accuracy of the rotation angle. Moreover, a stepping motor is selected to drive the combined type-hole seed-metering device. Others external affecting factors are also reduced. In this regard, stepping motors able to self-lock are selected to prevent rotation when non-system instruction after the system starts and improve the sowing quality. The system has self-protection function; thus, when the stepping motor is overloaded, the system stops sending pulse instructions to the stepping motor and starts the alarm device. The control flowchart is shown in Figure 6.

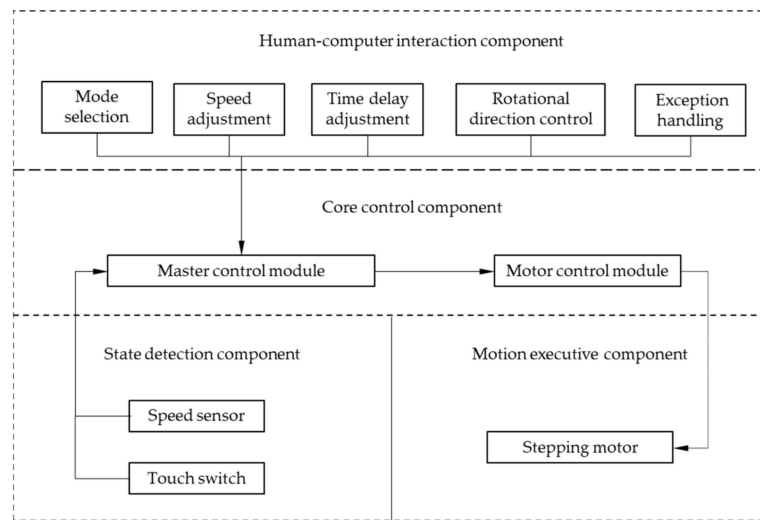


Figure 5. Schematic diagram of electronic control system.

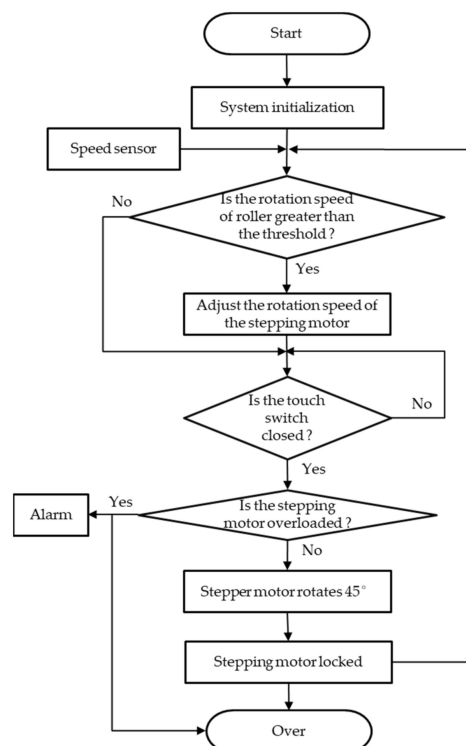


Figure 6. Control flow chart.

The system consists of a closed-loop control, where the rotation speed of the roller is obtained through the speed sensor in real-time. When the rotation speed exceeds or is lower than the preset range, the system adjusts the rotation speed of the stepping motor in real-time to arrange the sowing time and guarantee the filling performance of the combined type-hole seed-metering device.

A direct current voltage transducer was installed to provide power to the control box, stepping motor, and alert and speed sensors. The device obtains the direct current voltage from the battery of a tractor and converts it to the required voltage.

3. Materials and Methods

3.1. DEM Simulation

The kinematic and dynamic modelling of the device in the soil layer is complex; thus, it is difficult to perform a theoretical analysis. As a useful numerical computation approach, the DEM is increasingly being applied to the research between discrete units and machinery in agricultural mechanization production [26–28]. Therefore, this study adopted DEM to simulate the sowing process. In particular, the discrete element simulation software EDEM 2018 was used to perform the simulation experiments. The purpose of the DEM simulation is to establish the regression equation of sowing depth and determine the structure size of the telescopic pipe through the study of the sowing process.

3.1.1. Simulation Model and Parameters

The simplified solid assembly model of the dry direct-seeded rice with film mulching device was imported into the software preprocessing module, illustrated in Figure 7a. Multi-spherical polymerization was selected considering the characteristics of rice shapes, and a total of 25 sphere models with various diameters were connected to construct the rice particle model for the long and irregular shape of the rice (as shown in Figure 7b). The soil particle model considered spheres with diameters of 2 mm. The Hertz–Mindlin (no-slip) contact model included in EDEM was used for the simulation analysis, and the material physical and contact mechanical properties parameters are presented in Table 1.

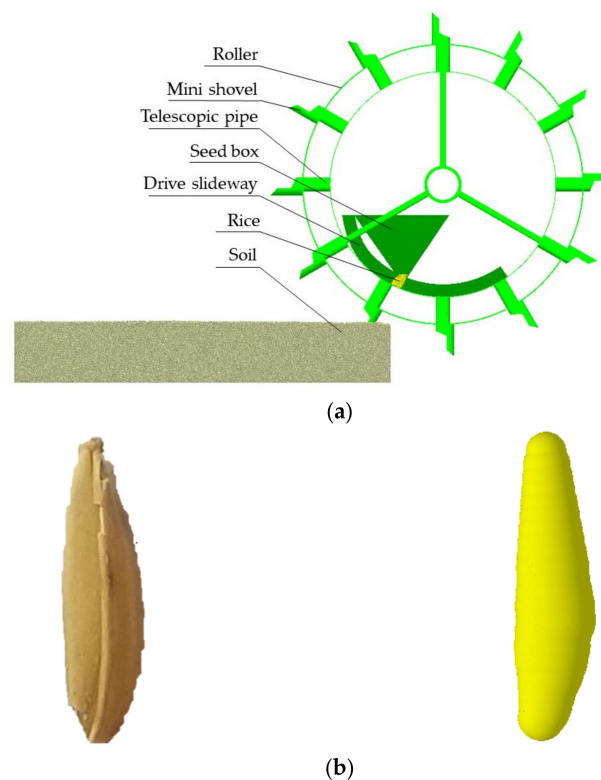


Figure 7. Simulation model: (a) The simplified model of the device; (b) Rice and rice particle model.

Table 1. Simulation experiments parameters.

Materials	Parameters	Value
Rice	Density ($\text{kg}\cdot\text{m}^{-3}$)	1147
	Poison ratio	0.25
	Shear modulus (Mpa)	108
Soil	Density ($\text{kg}\cdot\text{m}^{-3}$)	1914
	Poison ratio	0.38
	Shear modulus (Mpa)	1
Steel	Density ($\text{kg}\cdot\text{m}^{-3}$)	7850
	Poison ratio	0.3
	Shear modulus (Mpa)	79,000
Rice-Rice	Elastic restitution coefficient	0.13
	Static friction coefficient	0.52
	Rolling friction coefficient	0.1
Soil-Soil	Elastic restitution coefficient	0.11
	Static friction coefficient	0.6
	Rolling friction coefficient	0.4
Rice-Steel	Elastic restitution coefficient	0.41
	Static friction coefficient	0.48
	Rolling friction coefficient	0.01
Soil-Steel	Elastic restitution coefficient	0.12
	Static friction coefficient	0.3
	Rolling friction coefficient	0.05
Rice-Soil	Elastic restitution coefficient	0.08
	Static friction coefficient	0.9
	Rolling friction coefficient	0.7

3.1.2. Central Composite Design

According to the actual device shape and size, the particle factory was statically developed to form a soil tank of $600 \times 300 \times 150$ mm (length \times width \times height), the seeder working ground speed ranged from 0.4 to 0.6 m/s, and the fixed time step was set to 20% of the Rayleigh time step (8.86×10^{-7} s). A single simulation was run for 15 s to ensure the consistency of the sowing process.

In the simulation experiments, the forward speed of traction device (V), the extended length of the telescopic pipe (h_1), and the height of the lower oblique section of the telescopic pipe (h_2) were considered as the design variables, while the sowing depth (Y) was considered as the objective function. Preliminary combined factor experiments were conducted to determine the range of the experimental factors. The central composite design simulation experiment with three factors and three levels was performed using Design-Expert software [29], and the 0-level experiment was repeated five times. The code value of simulated experimental factors is shown in Table 2, while the simulation experiment scheme is shown in Table 3.

Table 2. Code of simulation experiment factors.

Code Value	Forward Speed V ($\text{m}\cdot\text{s}^{-1}$)	Extended Length h_1 (mm)	Height of the Lower Oblique Section h_2 (mm)
1	0.6	25	15
0	0.5	20	10
-1	0.4	15	5

Table 3. Simulation experiment scheme and results.

No.	Forward Speed V ($\text{m}\cdot\text{s}^{-1}$)	Extended Length h_1 (mm)	Height of the Lower Oblique Section h_2 (mm)	Sowing Depth Y (mm)
1	−1	−1	−1	18.8
2	1	−1	−1	23.6
3	−1	1	−1	27.9
4	1	1	−1	29.4
5	−1	−1	1	17.7
6	1	−1	1	21.5
7	−1	1	1	31.7
8	1	1	1	32.1
9	−1	0	0	22.5
10	1	0	0	24.6
11	0	−1	0	21
12	0	1	0	34.2
13	0	0	−1	26.1
14	0	0	1	26.9
15	0	0	0	25.8
16	0	0	0	26.3
17	0	0	0	22.7
18	0	0	0	23.7
19	0	0	0	26.3

3.2. Field Experiment

The working performance of the device for dry direct-seeded rice with film mulching was tested on 12 September 2020, in Gexinzhuang Village, Yilunbu Township, Renqiu City, Cangzhou City, Hebei Province ($38^{\circ}42'30''$ N, $116^{\circ}10'30''$ E, altitude 8 m). The qualified rate of sowing depth, the rate of empty seed, the qualified rate of seeds, the stagger rate, and the qualified rate of hole spacing, were investigated. In order to facilitate the observation of the operation effect of the device and the collection of data, the white polyethylene plastic film with a thickness of 0.01 mm was used in the field experiment. When sowing, the soil was soft, and the average soil compatibility of 100 mm soil layer was 283.5 kPa; the soil layer contained small quantities of soil blocks and stones; the soil moisture was 15.23%, which was slightly higher than the normal soil moisture during the seeding period. The tractor power was 29.42 kW. On average, there were 12 rice seeds in each hole. Before the field experiments, the rice precision seeder operating parameters were adjusted to achieve the optimal combination determined from the response surface optimization of the above simulation experiments: forward speed of tractor $V = 0.494$ m/s, the extended length of the telescopic pipe $h_1 = 15$ mm, and the height of the lower oblique section of the telescopic pipe $h_2 = 15$ mm. Three rows were sown, and a single row was 30 m in length. The field experiments were conducted in accordance with Chinese Agriculture Industrial Standard NY/T 987-2006 'Operating quality grain film-covering hill-drop drill' for data collection and device performance evaluation.

3.3. Data Analysis

The DEM simulation was focused on obtaining the sowing depth of different experimental combinations and establishing the response surface with the sowing depth as the response value. The images of the simulation results exported from the EDEM 2018 software were imported into CAD software to measure the sowing depth. The regression equation was analyzed through the variance and quadratic optimized. Data processing and analysis were performed using Microsoft Excel and Design Expert software.

4. Results and Discussion

4.1. Simulation Experimental Results

The results of the simulation experiments are shown in Table 3. The Quadratic model was used to establish the regression equation of the sowing depth. The results of the

analysis of variance for the regression equation showed a p -value of less than 0.0001. As a p -value greater than 0.05 indicates a lack of fit, the obtained regression equation is extremely significant; thus, the regression equation is effective. Among the three experimental factors, V is very significant, h_1 is extremely significant, and h_2 has a tiny effect. Regarding the interaction terms, only h_1 and h_2 items have a significant effect on the sowing depth, while the interaction of other terms is not significant. Concerning the quadratic term of factors, V^2 has a significant effect on sowing depth, while h_1^2 has an effect. After removing the terms with no effect, the regression equation of sowing depth was obtained by the quadratic optimization of the regression equation, as shown Equation (7), and the determination coefficient of the regression equation $R^2 = 0.9433$, and the adjustment determination coefficient $R^2_{adj} = 0.9072$. The variance analysis of the optimized regression equation is shown in Table 4.

$$Y = -29.745 + 253.572V - 1.789h_1 - 0.882h_2 - 1.65Vh_1 + 0.048h_1h_2 - 207.972V^2 + 0.0797h_1^2, \tag{7}$$

Table 4. ANOVA of the modified regression model for the central composite design.

Source	Sum of Squares	df	Mean Square	F-Value	p-Value
Model	329.28	7	47.04	26.14	<0.0001 *
V	15.88	1	15.88	8.82	0.0127 *
h_1	278.31	1	278.31	154.66	<0.0001 *
h_2	1.52	1	1.52	0.8453	0.3776
Vh_1	5.44	1	5.44	3.03	0.1098
h_1h_2	11.52	1	11.52	6.4	0.028 *
V^2	13.65	1	13.65	7.58	0.0188 *
h_1^2	12.53	1	12.53	6.96	0.023 *
Residual	19.79	11	1.8		
Lack of Fit	8.84	7	1.26	0.4612	0.8251
Pure Error	10.95	4	2.74		
Cor Total	349.08	18			

$R^2 = 0.9433$; $R^2_{adj} = 0.9072$; CV = 5.28%; Adequate precision = 17.8366; Note: * shows the term is significant ($p < 0.05$).

According to the requirements of agronomy, the sowing depth should be 15 to 25 mm. If the mean sowing depth is 20 mm, the target value is $Y=20$ mm. Subsequently, the optimal combination of $V = 0.494$ m/s, $h_1 = 15$ mm and $h_2 = 15$ mm was obtained by optimizing the regression equation. Simulation verification experiments (as shown in Figure 8.) were performed for the optimal combination under the target value; the average sowing depth was 21.35 mm, which was consistent with the predicted value.

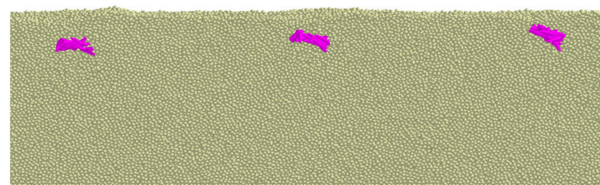


Figure 8. Simulation validation experiments of optimal combination.

4.2. Interactive Analysis and Discussion

According to the analysis of variance of the regression equation Equation (7), the following factors interact with each other: forward speed V , extended length h_1 , and height of the lower oblique section h_2 . The response surface analysis was conducted to account for the interaction between the factors. Three factors were considered; one factor was set to zero level to evaluate the interaction analysis between the two other factors. Figure 9 shows the response surface analysis.

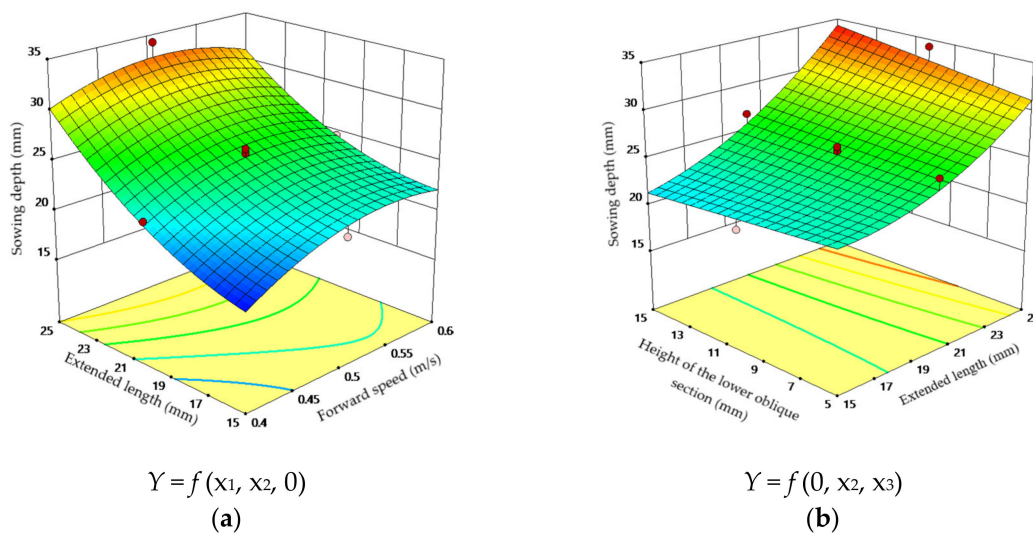


Figure 9. Interaction effect between factors: (a) Interaction between the forward speed and the extended length; (b) Interaction between extended length and height of the lower oblique section.

The response surface analysis of the interaction between the forward speed V and extended length h_1 is shown in Figure 9a. When the extended length h_1 was constant, the sowing depth increases with the forward speed V , and then the sowing depth tends to decrease. The maximum sowing depth occurs when the current feeding speed ranges from 0.5 to 0.55 m/s. This is because, as the forward speed V increases, the time when the telescopic pipe is in the soil decreases. Meanwhile, when the forward speed V is excessively high, the rice seeds cannot fall into the soil timely, and they would fall into the soil from the telescopic pipe during the excavation process, thus reducing the sowing depth. The sowing depth increases with the extended length h_1 . Furthermore, an increase in the sowing depth caused by the extended length h_1 is faster than that caused by the forward speed V . The extended length h_1 presents a more significant effect on the sowing depth than the other factors.

As shown in Figure 9b, when the extended length h_1 is constant, the sowing depth slightly increases with the height of the lower oblique section h_2 . The sowing depth increases with the extended length h_1 . The extended length h_1 increases rapidly and has a significant effect on the sowing depth, while the height of the lower oblique section h_2 does not present a significant effect on the sowing depth.

4.3. Field Experiment Results

On 12 September 2020, a field experiment was conducted with the experimental combination of $V = 0.494$ m/s, $h_1 = 15$ mm, and $h_2 = 15$. The experimental site was located at the experimental field of Hebei Zhengrong Agricultural machinery Manufacturing Company. The developed device and operation effects are shown in Figure 10.

As shown in Table 5, the experimental results indicate that the device has achieved the design objectives and the agronomic requirements of dry direct-seeded rice with film mulching.

Table 5. Experiment result statistics.

Parameters	Right Rate of Hill Distances/%	Stagger Rate of Film Hill and Hill/%	Right Rate of Depth of Sowing under Film/%	Right Rate of Seeds Per Hill/%	Rate of No Seed Hill/%
Value	100	4.8388	95	83.33	3.2258



Figure 10. Field experiments: (a) The developed device; (b) The effect of sowing.

5. Conclusions

Aimed at improving the technique of seeding in dry soil and drip irrigation for emergence, we proposed the combination seeding method of ‘mini shovel + telescopic pipe’ for dry direct-seeded rice with film mulching. The device for dry direct-seeded rice with film mulching was developed by theoretical calculation, DEM simulations, and field experiments. The research results showed that:

- (1) The precise rice sowing was obtained by selecting the combined type-hole seed-metering device. Moreover, the sowing depth can be adjusted within the range of 15 to 40 mm to satisfy the agronomic requirements of different sowing depths. The drive slideway converted passive sowing to forced sowing, and the mini shovel pushed away from the soil and obstacles in the seeding area, thus reducing the possibility that the telescopic pipe would be clogged.
- (2) DEM allowed the simulation of the device sowing process. Moreover, a regression equation was established with the sowing depth as the dependent variable, and the forward speed of the traction device, the extended length of the telescopic pipe, and the height of the lower oblique section of the telescopic pipe as the independent variables. The simulation experiments and field experiments showed that the regression equation could predict the sowing depth accurately.
- (3) Field experiments were conducted according to agronomic requirements. The experiment results showed that the right rate of hill distances, stagger rate of film hill and hill, right rate of depth of sowing under film, right rate of seeds per hill, and rate of no seed hill were 100%, 4.8388%, 95%, 83.33%, and 3.2258%, respectively. The experimental results showed that the rice precision seeder with trepanning in the plastic film could achieve the design and agronomic requirements for actual production.

The field experiments of the proposed precision seeder achieved the desired effect; however, the sample size and scope of the field experiments are not substantial enough to understand the adaptability of the device to different regions and soil environments. The adaptability of the device should be verified in the future.

Author Contributions: Methodology, H.L. and W.Y.; software, H.L. and L.F.; validation, W.Y. and S.Z.; formal analysis, X.L.; investigation, H.L. and Z.L.; data curation, H.L.; writing—original draft preparation, H.L.; writing—review and editing, W.Y. and S.Z.; visualization, H.L.; supervision, W.Y.; project administration, W.Y.; funding acquisition, W.Y. and S.Z. All authors have read and agreed to the published version of the manuscript.

Funding: This research was funded by the National Key R & D Program (2018YFD0200700, 2017YFD0700704, and 2016YFD0200606) and Special Projects in Key Area of ‘Artificial Intelligence’ of General Colleges and Universities in Guangdong Province (2019KZDZX1003).

Institutional Review Board Statement: Not applicable.

Informed Consent Statement: Not applicable.

Data Availability Statement: The data presented in this study are available on demand from the first author at (lihui17@mails.jlu.edu.cn).

Acknowledgments: The authors would like to thank the technical support of the teacher and supervisor. We also appreciate the assistance provided by team members during the experiments. Moreover, we would like to thank Hebei Zhengrong Agricultural machinery Manufacturing Company for providing the device manufacturing. Additionally, we sincerely appreciate the work of the editor and the reviewers of the present paper.

Conflicts of Interest: The authors declare no conflict of interest.

References

- Kumar, V.; Ladha, J.K. Direct Seeding of Rice: Recent Developments and Future Research Needs. *Adv. Agron.* **2011**, *111*, 297–413. [[CrossRef](#)]
- Tuong, T.; Bouman, B. Rice production in water scarce environments. In *Water Productivity in Agriculture: Limits and Opportunities for Improvement*; Kijne, J., Barker, R., Molden, D., Eds.; CABI Publishing: Wallingford, UK, 2003; pp. 53–67.
- Chakraborty, D.; Ladha, J.K.; Rana, D.S.; Jat, M.L.; Gathala, M.K.; Yadav, S.; Rao, A.N.; Ramesha, M.S.; Raman, A. A global analysis of alternative tillage and crop establishment practices for economically and environmentally efficient rice production. *Sci. Rep.* **2017**, *7*, 9342. [[CrossRef](#)] [[PubMed](#)]
- Tuong, T.P.; Castillo, E.G.; Cabangon, R.C.; Boling, A.; Singh, U. The drought response of lowland rice to crop establishment practices and N-fertilizer sources. *Field Crop. Res.* **2002**, *74*, 243–257. [[CrossRef](#)]
- Sun, L.M.; Hussain, S.; Liu, H.Y.; Peng, S.B.; Huang, J.L.; Cui, K.H.; Nie, L.X. Implications of low sowing rate for hybrid rice varieties under dry direct-seeded rice system in central China. *Field Crop. Res.* **2015**, *175*, 87–95. [[CrossRef](#)]
- Farooq, M.; Siddique, K.H.; Rehman, H.; Aziz, T.; Lee, D.J.; Wahid, A. Rice direct seeding: Experiences, challenges and opportunities. *Soil Tillage Res.* **2011**, *111*, 87–98. [[CrossRef](#)]
- Liu, H.Y.; Hussain, S.; Zheng, M.M.; Peng, S.B.; Huang, J.L.; Cui, K.H.; Nie, L.X. Dry direct-seeded rice as an alternative to transplanted-flooded rice in Central China. *Agron. Sustain. Dev.* **2015**, *35*, 285–294. [[CrossRef](#)]
- Sandhu, N.; Subedi, S.R.; Singh, V.K.; Sinha, P.; Kumar, S.; Singh, S.P.; Ghimire, S.K.; Pandey, M.; Yadav, R.B.; Varshney, R.K.; et al. Deciphering the genetic basis of root morphology, nutrient uptake, yield, and yield-related traits in rice under dry direct-seeded cultivation systems. *Sci. Rep.* **2019**, *9*, 9334. [[CrossRef](#)]
- Xu, L.; Li, X.X.; Wang, X.Y.; Xiong, D.L.; Wang, F. Comparing the Grain Yields of Direct-Seeded and Transplanted Rice: A Meta-Analysis. *Agronomy* **2019**, *9*, 767. [[CrossRef](#)]
- Kakumanu, K.R.; Kotapati, G.R.; Nagothu, U.S.; Kuppanan, P.; Kallam, S.R. Adaptation to climate change and variability: A case of direct seeded rice in Andhra Pradesh, India. *J. Water Clim. Chang.* **2019**, *10*, 419–430. [[CrossRef](#)]
- Fawibe, O.O.; Hiramatsu, M.; Taguchi, Y.; Wang, J.; Isoda, A. Grain yield, water-use efficiency, and physiological characteristics of rice cultivars under drip irrigation with plastic-film-mulch. *J. Crop Improv.* **2020**, *34*, 414–436. [[CrossRef](#)]
- Zhang, Z.C.; Zhang, S.F.; Yang, J.C.; Zhang, J.H. Yield, grain quality and water use efficiency of rice under non-flooded mulching cultivation. *Field Crop. Res.* **2008**, *108*, 71–81. [[CrossRef](#)]
- He, H.B.; Ma, F.Y.; Yang, R.; Chen, L.; Jia, B.; Cui, J.; Fan, H.; Wang, X.; Li, L. Rice Performance and Water Use Efficiency under Plastic Mulching with Drip Irrigation. *PLoS ONE* **2013**, *8*, e83103. [[CrossRef](#)] [[PubMed](#)]
- Jabran, K.; Ullah, E.; Hussain, M.; Farooq, M.; Zaman, U.; Yaseen, M.; Chauhan, B.S. Mulching Improves Water Productivity, Yield and Quality of Fine Rice under Water-saving Rice Production Systems. *J. Agron. Crop Sci.* **2015**, *201*, 389–400. [[CrossRef](#)]
- Li, Y.S.; Wu, L.H.; Zhao, L.M.; Lu, X.H.; Fan, Q.L.; Zhang, F.S. Influence of continuous plastic film mulching on yield, water use efficiency and soil properties of rice fields under non-flooding condition. *Soil Tillage Res.* **2007**, *93*, 370–378. [[CrossRef](#)]
- Wang, Z.M.; Luo, X.W.; Chen, X.F.; Mo, Z.W. Effects of precision rice hill-drop drilling on rice quality. *Trans. Chin. Soc. Agric. Eng.* **2015**, *31*, 16–21. [[CrossRef](#)]
- Wang, Z.M.; Dai, Y.Z.; Wang, B.L.; Zhang, M.H.; Chen, X.F.; Mo, Z.W.; Luo, X.W. Research on Hill-drop Drilling and Row Drilling of Rice. *China Rice* **2016**, *22*, 19–20. [[CrossRef](#)]
- Wang, J.P. Study of Framework and Parameter of Film Mulching Hill-Drop Planter. Master's Thesis, China Agriculture University, Beijing, China, 2005.
- Zhang, S.J. Design and test of 2BMK-1/3 dibble filming planter machine. *J. Chin. Agric. Mech.* **2013**, *34*, 113–117. [[CrossRef](#)]
- Niu, Q.; Wang, S.G.; Chen, X.G. Design of Rice Planter with Plastic Film Mulched Drip Irrigation. *Trans. Chin. Soc. Agric. Mach.* **2016**, *47*, 102. [[CrossRef](#)]
- Luo, X.W.; Wang, Z.M.; Jiang, E.C.; Li, J.H.; Li, Q.; Chen, W.T. Design of Disassemble Rubber Guard Device for Cell Wheel Feed. *Trans. Chin. Soc. Agric. Mach.* **2008**, *39*, 60–63.
- Zhang, M.H.; Luo, X.W.; Wang, Z.M.; Dai, Y.Z.; Wang, B.L.; Zheng, L. Design and Experiment of Combined Hole-type Metering Device of Rice Hill-drop Drilling Machine. *Trans. Chin. Soc. Agric. Mach.* **2016**, *47*, 29–36.

23. Liu, H.X.; Su, H.; Li, J.L.; Liu, Z.J. Interactive Optimal Design System of Drum-type No-till Planter Mechanism. *Trans. Chin. Soc. Agric. Mach.* **2019**, *50*, 58–68.
24. Liu, H.X.; Wen, H.N.; Gai, G.W.; Tang, S.F. Design and Experiment on Passive Drum-type No-till Planter Cavitation Mechanism. *Trans. Chin. Soc. Agric. Mach.* **2017**, *48*, 53–61. [[CrossRef](#)]
25. Zhang, X.J.; Yang, Y.; Zhou, L. Selection and definitiveness on main parameters of bunch planting cylinder. *Trans. Chin. Soc. Agric. Mach.* **1998**, *29*, 63–66.
26. Shi, Y.Y.; Sun, X.; Wang, X.C.; Hu, Z.C.; Newman, D.; Ding, W.M. Numerical simulation and field tests of minimum-tillage planter with straw smashing and strip laying based on EDEM software. *Comput. Electron. Agric.* **2019**, *166*, 105021. [[CrossRef](#)]
27. Barr, J.; Desbiolles, J.; Ucgul, M.; Fielke, J.M. Bentleg furrow opener performance analysis using the discrete element method. *Biosyst. Eng.* **2020**, *18*, 99–115. [[CrossRef](#)]
28. Li, M.S.; Mitsuoka, M.; Inoue, E.; Ye, J.; Liu, J.; Yang, S.; Zeng, B.G.; Song, X.X.; Okayasu, T.; Hirai, Y. Design and Performance Analysis of a Seed Metering Device for a Buckwheat Seeder Adopting Discrete Element Analysis. *J. Fac. Agric. Kyushu Univ.* **2020**, *65*, 123–129. [[CrossRef](#)]
29. Ge, Y. *Experimental Design Method and Application of Design-Expert Software*; Harbin Institute of Technology Press: Harbin, China, 2015; pp. 62–95.